scientific reports

Check for updates

OPEN

The role of thrombospondin-1 in trehalose-induced autophagy and ocular hypertension in mice

Choi-ying Ling[1,9], Kit-ying Choy[1,2,9], Hoi-lam Li[3], Choi-yee Tse[1], Wei-ying Yang[1], Nga-wai Wong[1], W. Daniel Stamer[4,5], Chi-wai Do[1,2,6,7], Dennis Yan-yin Tse[1,2,6,8]✉ & Samantha Sze-wan Shan[1,2,6,8]✉

Prolonged use of dexamethasone (DEX) increases intraocular pressure (IOP) and the risk of glaucoma. Recent studies have shown that DEX upregulates thrombospondin-1 (*THBS1*) gene expression and induces dysregulation of macroautophagy/autophagy in primary human trabecular meshwork (hTM) cells. Trehalose, a natural disaccharide, activates autophagy and protects cells against environmental stresses. Here, we report that trehalose-induced autophagy enhanced outflow facility, reduced IOP, and protected against ocular hypertension in mice. We analyzed autophagy induction by trehalose in hTM cells. Our data demonstrated that trehalose transcriptionally upregulated prototypical autophagy related genes and activated autophagy through the downregulation of *THBS1*. Consistent with prior findings, the results indicated that *THBS1* silencing or inhibition is a key cellular event for the regulation of aqueous humor outflow and IOP homeostasis. In conclusion, this study identified trehalose-induced autophagy as a protective mechanism against ocular hypertension which may have therapeutic potential.

Keywords Autophagy, Intraocular pressure, Ocular hypertension, Outflow facility, Thrombospondin-1, Trehalose

Abbreviations

AP	autophagosome AST: aspartate aminotransferase
ATGs	autophagy-related genes
ATG5	autophagy-related protein 5
ATG7	autophagy related 7
DEX	dexamethasone
ECM	extracellular matrix
hTM	human trabecular meshwork
IOP	intraocular pressure
i.p.	intraperitoneal
LC3	microtubule-associated protein 1 light chain 3
NFE2L2	nuclear factor, erythroid derived 2, like 2
PRED	prednisolone
Rapa	rapamycin
RGCs	retinal ganglion cells
siCtl	negative control siRNA
siTHBS1	THBS1-siRNA
SQSTM1	sequestosome 1
TGFB	transforming growth factor beta
THBS1	thrombospondin-1

[1]School of Optometry, The Hong Kong Polytechnic University, Hong Kong, China. [2]Centre for Eye and Vision Research (CEVR), 17W Hong Kong Science Park, Hong Kong, China. [3]Ophthalmology, Boston University Chobanian & Avedisian School of Medicine, Boston, MA, USA. [4]Department of Ophthalmology, Durham, NC, USA. [5]Department of Biomedical Engineering, Duke University, Durham, NC, USA. [6]Research Centre for SHARP Vision (RCSV), The Hong Kong Polytechnic University, Hong Kong, China. [7]Research Institute of Smart Ageing (RISA), The Hong Kong Polytechnic University, Hong Kong, China. [8]School of Optometry, The Hong Kong Polytechnic University, Hong Kong, China. [9]These authors jointly supervised this work: Choi-ying Ling and Kit-ying Choy. ✉email: dennis.tse@polyu.edu.hk; samantha.shan@polyu.edu.hk

TM	trabecular meshwork
TOR	target of rapamycin

The Global Data on Visual Impairment 2010 reports that glaucoma is the second most common cause of blindness, accounting for 8% of cases worldwide[1]. Increasing life expectancy is believed to contribute to glaucoma prevalence, with approximately 111.8 million people globally estimated to be affected by glaucoma in 2040[2], which poses a substantial burden to healthcare systems. Visual impairment and blindness cause severe disability, impair activities of daily life, reduce the quality of life, and increase the risk of injury and death of affected patients. Known as "the thief of sight", glaucoma is typically asymptomatic for affected patients during the early stages of the disease, because the subtle and gradual loss in peripheral vision is usually not noticed by the patients. Without proper treatment, vision will further deteriorate, and the eventual outcome may be irreversible blindness.

Glaucoma is an optic neuropathy associated with the loss of retinal ganglion cells (RGCs). Elevated IOP is a major risk factor for glaucoma[3,4], and the main parameter targeted by therapeutic interventions. Trabecular meshwork (TM) cell dysfunction and extracellular matrix (ECM) protein deposition cause a decrease in conventional outflow facility[5], resulting in elevated IOP, ultimately contributing to glaucoma. One common type of glaucoma is caused by prolonged corticosteroid treatment, such as DEX, which leads to IOP elevation and optic nerve damage if left untreated[6,7]. Similar to glaucoma generally, DEX reduces conventional outflow facility by causing some pathological changes in TM and Schlemm's canal (SC). DEX increases the production of ECM proteins, including glycosaminoglycans, fibronectin and collagens[8–10], and prevent their degradation by decreasing metalloproteinases expression[11,12]. DEX also induces cross-linked actin networks (CLANs)[13–15] and increases TM stiffness[14], leading to increased outflow resistance and IOP[16]. DEX-treated mice eyes show increased collagen[17] along the inner wall endothelium of SC, with increased basement membrane length and continuity[17,18]. In a recent study, we showed that DEX and prednisolone alter the alpha-actin cytoskeletal architecture of cultured primary hTM cells[19]. Moreover, using a proteomic approach, we showed that protein levels of THBS1, an activator of transforming growth factor beta (TGFB)[20], are increased following treatment with corticosteroids. In contrast, we showed that Y39983, a Rho-kinase inhibitor, leads to *THBS1* downregulation in hTM cells[21]. In addition, a *THBS1*-inhibitory peptide significantly increases outflow facility in mouse eyes[19]. These strongly suggest that reduced *THBS1* expression is a key cellular event for increasing outflow facility.

In 2021, Sbardella et al. reported that exposure of TM cells to DEX inhibits the autophagosome (AP) biogenesis pathway[22], which, along with other studies[23,24], suggests that autophagy dysregulation in TM cells contributes to elevated IOP in steroid-induced glaucoma. Autophagy is a cellular catabolic process in which cellular components are degraded by the lysosomal machinery for cellular homeostasis with macroautophagy being the most-studied form characterized by AP formation[25]. Dysregulation of autophagy has been associated with age-related diseases and neurodegenerative disorders[26–28], including glaucoma[23,29–34]. Recent studies have shown that autophagy inducers like rapamycin protect TM cells from oxidative stress and apoptosis[23]. A decrease in autophagic activity may contribute to age-related progressive failure of TM cellular functions and the pathogenesis of primary open angle glaucoma[33], while mechanical stress from elevated IOP can activate autophagy in TM cells[34].

In the current study, we evaluated the role of autophagy in hTM cells which were modulated pharmacologically by the prototypical autophagy inducer trehalose. We characterized the role of autophagy in hTM morphology, ECM production, aqueous humor outflow facility, and IOP. Trehalose, a natural disaccharide, is in use for topical and systemic treatment of ocular and systemic disorders, including oculopharyngeal muscular dystrophy, atherosclerosis, and dry eyes[35,36]. Upregulation of autophagy by trehalose has been reported previously[37,38]. However, to our knowledge the effect of trehalose on IOP, aqueous humor flow, and ECM deposition in the TM have not been previously characterized. We performed a comprehensive in vitro and in vivo characterization of the effects of trehalose to support the hypothesis that autophagy induction reduced IOP and provided a rationale for testing autophagy enhancers in clinical studies with glaucoma patients.

Materials and methods

Outflow facility measurement

Adult C57BL/6J mice (2–4 months old) were used. Throughout the experiment, ex vivo mouse eyes were continuously perfused with HEPES buffered Ringer's solution containing 113 mM NaCl, 4.56 mM KCl, 21 mM $NaHCO_3$, 0.6 mM $MgSO_4 \cdot 7H_2O$, 7.5 mM D-glucose, 1 mM Re-glutathione, 1mM $Na_2HPO_4 \cdot 12H_2O$, 10 mM HEPES, and 1.4 mM $CaCl_2 \cdot 2H_2O$, supplemented with either trehalose (50 mM or 100 mM) or vehicle control (PBS). For perfusions, the anterior chambers of paired mouse eyes were cannulated by a 33-gauge needle (World Precision Instruments). The needle was connected via a pressure transducer (Honeywell) to a glass syringe (Hamilton) filled with Ringer's solution at 37 °C and placed on a motorized syringe pump (Harvard Apparatus) under computer control. Sequential pressure steps of 4, 8, 12, and 16 mmHg were used. A stable perfusion rate was obtained at each pressure step for at least 10 min. The outflow facility measurement lasted about 4 h, including the equilibration time of about 30 min. The outflow facility was then derived from the average flow rate calculated at each perfusion pressure during the stable perfusion period. All procedures performed were in accordance with the ARVO Statement for the Use of Animals in Ophthalmic Vision and Research and ARRIVE guidelines. Approval was granted by the Animal Subjects Ethics Sub-Committee (ASESC) of the Hong Kong Polytechnic University (Date: 2023 February 07/ASESC Case No.: 21–22/91-SO-R-GRF).

Animal Preparation and non-invasive IOP measurements

Adult C57BL/6J mice were used and kept in cages with 12-hour light/dark cycles daily. To study the intervention of trehalose through intraperitoneal (i.p.) injection or topical application, mice were divided into 2 treatment groups for each administration route. In each treatment group, mice were further divided into 2 subgroups: the trehalose treatment group and the vehicle control group. For the i.p. group, 0.2 ml of trehalose (1 mg/g) or vehicle control (PBS) was injected once every 2 days in the morning for 2 weeks. For the topical application group, 8 µl of trehalose (1 M) or vehicle control was administered for 3 h. The IOP was measured with a Tonolab rebound tonometer (Icare) before and after treatment under awake conditions. After the experiment, animals were euthanized humanely with overdose of Ketamine-Xylazine (at least 3 times of anaesthetic dose: 100 mg/kg Ketamine and 10 mg/kg Xylazine) by i.p. Comparisons between trehalose-treated and vehicle control groups were performed.

Primary hTM cell culture

The hTM cells were obtained from the Department of Ophthalmology, the Duke University School of Medicine (Durham, NC). The isolation of hTM cells was performed as described in previous studies[39–41] and authenticated according to consensus recommendations[42]. The hTM cells were plated and incubated at 37 °C with low-glucose DMEM containing 10% FBS until confluent. Subsequently, they were maintained in low-glucose DMEM containing 1% FBS for at least a week before the assays described below.

Western blot analysis

The hTM cells were lysed in lysis buffer, containing 7 M Urea, 2 M Thiourea, 30 mM TRIS, 1% ASB14 (Calbiochem), 2% CHAPS and protease inhibitor cocktail, and sonicated for 1 h on ice, followed by centrifugation at 13,000 × g for 20 min. After collecting the supernatants, total proteins were quantified by the Bio-Rad Protein Assay. The hTM protein (25 µg) was mixed with SDS loading buffer, heated at 95 °C for 5 min, separated in a 7% SDS-PAGE gel, and transferred into a PVDF membrane (Bio-Rad Laboratories). The PVDF membrane was incubated with anti-THBS1 primary antibody (1:500, R and D systems) or anti-LC3B primary antibody (1:2000, Abcam) at 4 °C overnight. After washing, the membrane was incubated with anti-goat IgG conjugated with horseradish peroxidase (1:2000, Thermo Fisher Scientific). Anti-GAPDH antibody (1:5000, Calbiochem) was used as a loading control. The protein expressions were then visualized by the Pierce SuperSignal West Pico Chemiluminescent substrate (Thermo Fisher Scientific). Quantification of band intensity was performed using ImageJ (version 1.54 m; https://imagej.net/).

Real time-quantitative polymerase chain reaction (RT-qPCR)

The total RNA of hTM cells was extracted and quantified using the Qiagen RNeasy Micro Kit (Qiagen). Reverse transcription of mRNA to cDNA was performed using the High-Capacity cDNA Reverse Transcription Kit (Thermo Fisher Scientific), followed by qPCR using the LightCycler 480 SYBR Green I Master (Roche Applied Science) with primers specific for the target genes: autophagy-related protein 5 (*ATG5*; forward, 5'-AAGCTGTTTCGTCCTGTGGC-3'; reverse, 5'-CCGGGTAGCTCAGATGTTCA-3'), autophagy related 7 (*ATG7*; forward, 5'-CGTTGCCCACAGCATCATCTTC-3'; reverse, 5'-TCCCATGCCTCCTTTCTGGTTC-3'), Nuclear factor, erythroid derived 2, like 2 (*NFE2L2*; forward, 5'-ACACGGTCCACAGCTCATC-3'; reverse, 5'-TGTCAATCAAATCCATGTCCTG-3'), sequestosome 1 (*SQSTM1*; forward, 5'-TGCCCAGACTACGACTTGTG-3'; reverse, 5'-AGTGTCCGTGTTTCACCTTCC-3'), connective tissue growth factor *(CTGF*; forward, 5'-CAGAGCAGCTGCAAGTACCA-3'; reverse, 5'-GCCAAACGTGTCTTCCAGTC-3'), *THBS1* (forward, 5'-CGTCCTGTTCCTGATGCATG-3'; reverse, 5'-CCAGGAGAGCTTCTTCCACA-3'), and the internal reference gene, *GAPDH* (forward, 5'-GATTTGGTCGTATTGGGCGC-3'; reverse, 5'-TGGACTCCACGACGTACTCA-3'). qPCR was performed in 96-well plates on the ROCHE LightCycler 480 (Roche Applied Science). In each 10 µl reaction, 1x Taq PCR Master Mix, 2 µl cDNA template and 10 µM primers (forward and reverse primers, respectively) were used. The thermal cycling conditions were 95 °C for 5 min, followed by 40 cycles of 95 °C for 30 s, 61 °C for 30 s, and 72 °C for 30 s. A melting-curve analysis was performed to rule out primer–dimer formation and non-specific product amplification. A negative control sample without a template was included on each plate. Data were analyzed using LightC480 software (version: 1.5.1.62; http://www.lightcycler.com).

Downregulation of THBS1 by SiRNA

Gene silencing was performed using a THBS1-siRNA (siTHBS1; Thermo Fisher Scientific), and a non-silencing siRNA (siCtl; Thermo Fisher Scientific), as a negative control. The non-silencing siRNA had no known homology to other mammalian genes. As described in our previous study, 100 pmol siRNAs were transfected into hTM cells using Lipofectamine 3000 transfection reagent (Invitrogen)[21]. After 24-hour incubation, the cells were processed for RT-qPCR.

Autophagic vacuole quantification assay

An autophagy assay kit (Abcam, to investigate the relevance of THBS1 in autophagy in hTM cells in the presence of trehalose and 2 THBS1 inhibitor peptides. The LSKL peptide (AnaSpec) is a selective THBS1 inhibitor which inhibits THBS1-mediated TGFB activation while the SLLK peptide (AnaSpec) is a THBS1 inhibitor scramble peptide serving as a control. The hTM cells were either incubated individually with trehalose (100 mM), SLLK or LSKL peptide (1 or 5 µM), or co-incubated with both trehalose and LSKL peptide for 48 h. Autophagic vacuoles were labeled according to the instructions of the manufacturer of the autophagy assay kit. The assay selectively labels autophagic vacuoles with a fluorescent dye, and the fluorescent intensity of cells was quantified using a BD Accuri C6 Flow Cytometer (BD Bioscience).

Statistical analysis

Statistical analysis was tested with Student's t-test or two-way repeated measures ANOVA with Bonferroni test, as appropriate. P-values below 0.05 were considered statistically significant.

Results

Trehalose increased outflow facility and reduced IOP

Trehalose is considered safe and well tolerated in humans and animals with low potential cytotoxicity[43]. To investigate the role of trehalose in IOP homeostasis, we administered trehalose (1 mg/g, $n = 13$) via i.p. injection (0.2 ml) to adult C57BL/6J mice, a dosage of which did not cause any systemic or ocular toxicity to the mice (Supplementary Fig. S1). After 2 weeks of treatment, trehalose significantly reduced IOP by 9.4% (at day 14, $P = 0.0066$; Fig. 1a) relative to vehicle control ($n = 13$). In parallel studies, we observed that topical application of trehalose (1 M in 8 µl, $n = 5$) significantly reduced IOP by 19.7% ($P = 0.0037$; Fig. 1b) at 3 h when compared with vehicle control ($n = 6$). As the topically applied drug has a lower capacity to penetrate the cornea, a higher concentration of trehalose (1 M) without causing any cytotoxicity and gross structural changes to the animals (Supplementary Fig. S2) was used. To determine if the IOP decrease was due to effects on the conventional outflow, we continuously perfused 50 mM trehalose, 100 mM trehalose, or PBS (vehicle control) in ex vivo eyes from adult male C57BL/6J mice and monitored the outflow facility using perfusion system. Both 50 mM and 100 mM trehalose increased the outflow facility by 69.4% ($P = 0.0144$; Fig. 1c) and 49.3% ($P = 0.0290$; Fig. 1d), respectively after 4 h of perfusion, when compared with vehicle control ($n = 6$). These results strongly supported the role of trehalose in regulating IOP homeostasis.

Trehalose increased LC3-II protein expression and autophagy-associated gene expressions

To confirm whether trehalose induces autophagy in hTM cells, we examined the expression of key autophagy-associated proteins and genes in trehalose-treated hTM cells. Microtubule-associated protein 1 light chain 3 (LC3) is abundantly localized at the autophagosomal membranes[44], where LC3 is activated into LC3-I,

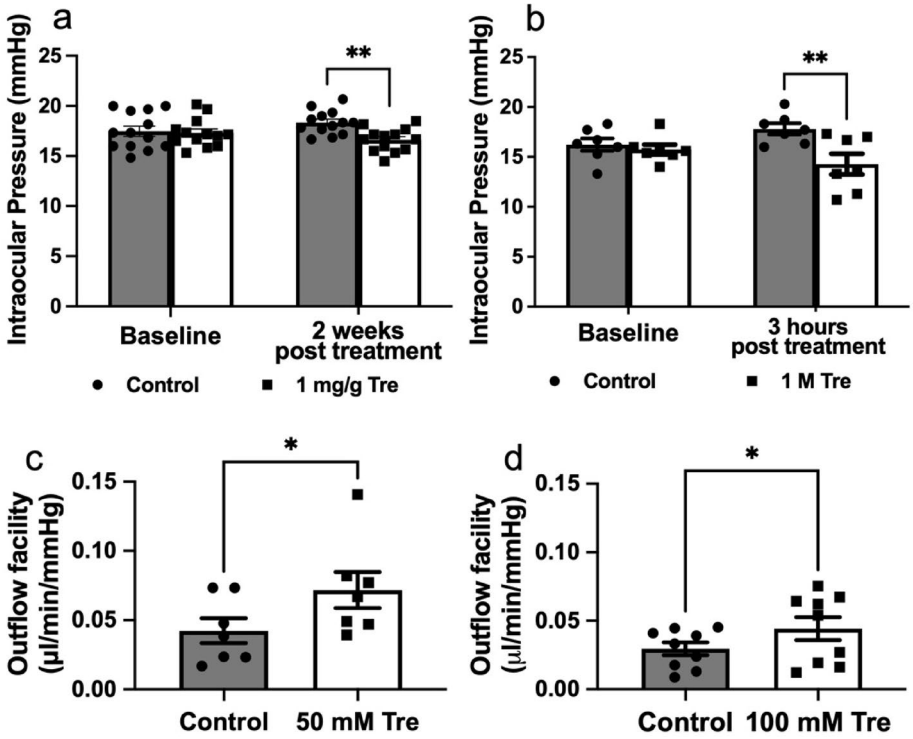

Fig. 1. Trehalose reduced IOP and increased outflow facility in enucleated eyes from adult C57BL/6J mice. (**a**) In adult C57BL/6J mice, 1 mg/g trehalose ($n = 13$) or vehicle (PBS)-control ($n = 13$) was administered by i.p. once every 2 days. IOP was significantly reduced by 9.4% ($P = 0.0066$; two-way repeated measures ANOVA with Bonferroni test) at 2 weeks after trehalose administration. (**b**) In adult C57BL/6J mice, 1 M trehalose ($n = 7$) or vehicle control ($n = 7$) was administered by topical application. IOP was significantly reduced by 19.7% ($P = 0.0037$; two-way repeated measures ANOVA with Bonferroni test) at 3 h after trehalose application. (**c**) In ex vivo perfused eyes from adult C57BL/6J mice, 50 mM trehalose increased the outflow facility by 69.4% ($P = 0.0144$; paired Student's t-test) compared to the vehicle control ($n = 7$) after 4 h of perfusion. (**d**) 4-hour perfusion of 100 mM trehalose increased the outflow facility by 49.3% ($P = 0.0290$; paired Student's t-test) compared to the vehicle control ($n = 9$). The data represent the mean ± standard error of the mean (SEM). Statistical significance relative to vehicle control is indicated by *($P < 0.05$) and **($P < 0.01$). Tre: trehalose.

conjugated with phosphatidylethanolamine to form LC3-II[44,45]. Measuring the amount of LC3-II allows for reliable quantification of AP and autophagy-related structures, making it the most widely used key AP marker[46]. In our experiments, 100 mM of trehalose, a concentration that had no adverse effects on cell morphology and viability (Supplementary Fig. S3), increased LC3-II protein expression in hTM cells (1.8-fold; $P = 0.0421$; Fig. 2a and b), indicating that trehalose-induced autophagy in hTM cells.

Autophagy is driven by key autophagy-related genes (ATGs). Among these genes, *ATG5* and *ATG7* are the essential genes for autophagy due to their roles in mediating the conjugation of phosphatidylethanolamine to LC3[44]. *ATG5* and *ATG7* expression levels were upregulated by 1.5- ($P = 0.0290$) and 1.4-fold ($P = 0.0201$), respectively, in trehalose-treated hTM cells (Fig. 2c and d). *NFE2L2* is a transcription factor regulating many genes for cellular homeostasis, including *ATG5* and *ATG7* for autophagy[47–49]. It also upregulates a wide range of antioxidant gene transcription to attenuate oxidative stress in mitochondria[50]. Forty-eight hours of trehalose treatment induced the upregulation of *NFE2L2* expression by 2.8-fold ($P = 0475$; Fig. 2e) in hTM cells. These results further confirmed that trehalose induced autophagy in hTM cells.

LC3 selectively binds to its specific substrate, SQSTM1, to recruit ubiquitinated proteins and mediate selective autophagic degradation[51,52]. In general, SQSTM1 protein levels inversely correlate with autophagic activity and accumulate in autophagy-deficient cells[53,54]. However, in mouse embryonic fibroblasts the autophagy-induced decrease in SQSTM1 is most pronounced 2 h after starvation and recovers afterwards[55]. In our experiments, after forty-eight hours of treatment with trehalose, expression of *SQSTM1* increased by 2.6-fold in hTM cells ($P = 0.029$; Fig. 2f). The increased expression of *SQSTM1* observed in our trehalose-treated cells might be due to the forty-eight-hour starvation period of trehalose treatment. Moreover, SQSTM1 is an inducer of NFE2L2, and the high level of SQSTM1 may activate NFE2L2 for the upregulation of *ATG5* and *ATG7* expression[49].

Trehalose-induced autophagy through reducing THBS1 expression and function in hTM cells

THBS1 is a prominent ECM protein in the TM[56] and an activator of TGFB[20]. We have shown that corticosteroids, compounds that are known for increasing IOP, upregulate THBS1 in hTM cells[19] while the addition of THBS1 inhibitory peptide increases outflow facility in mice eyes[21], indicating that THBS1 expression and function are essential for regulating outflow facility and, thus, IOP. In this study, trehalose significantly reduced both mRNA ($P = 0.0028$; Fig. 3a) and protein levels ($P = 0.0055$; Fig. 3b and c) of THBS1 in hTM cells by at least 50%. 4-hour perfusion of trehalose also reduced THBS1 protein level in mouse TM tissue (Supplementary Fig. S6). All these findings suggested that THBS1 played an instrumental role in regulating autophagy-induced outflow facility.

To investigate the relevance of THBS1 in trehalose-induced autophagy in hTM cells, we studied the effects of trehalose on autophagy-associated gene expression in *THBS1* siRNA-silenced hTM cells. Consistent with our

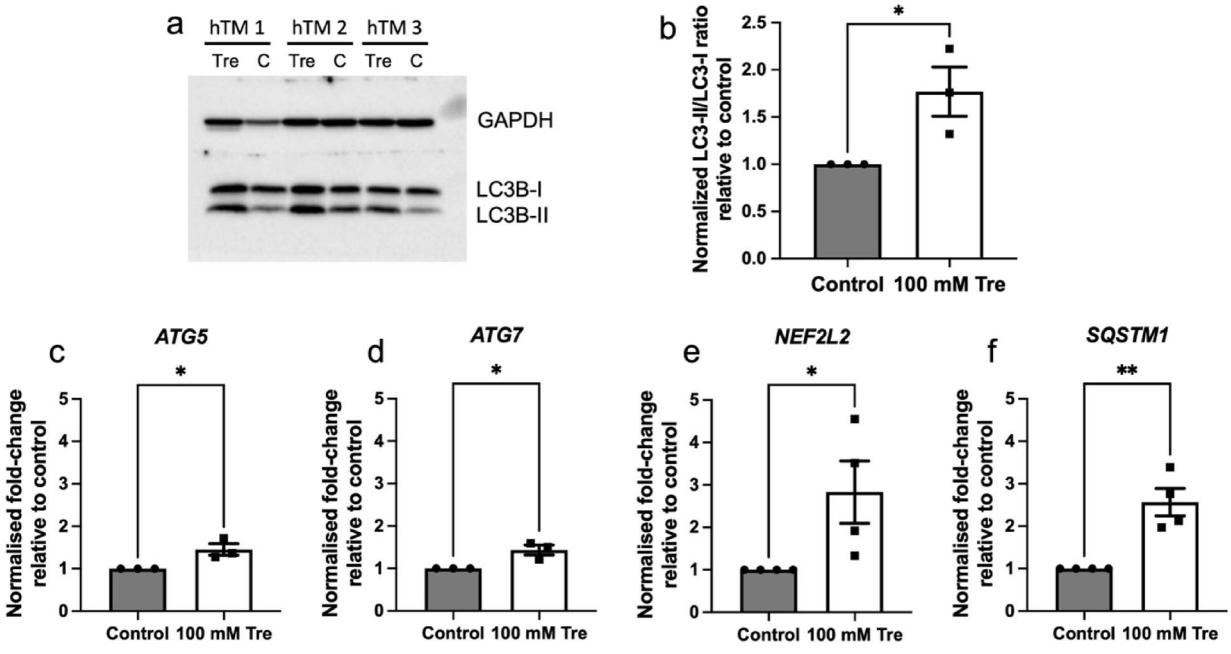

Fig. 2. Trehalose increased LC3-II protein expression and autophagy-associated genes expression in hTM cells. Cultured hTM cells were treated with 100 mM trehalose and vehicle controls in serum-free medium for 48 h. Protein expression of LC3-II was analyzed by western blot. (**a**) Representative of three individual western blots of LC3-II expression in hTM cells. The original blot is presented in Supplementary Fig. S4. (**b**) The ratio of LC3-II: LC3-I protein level ($n = 3$ different cell strains) as shown in (**a**). The gene expression levels of (**c**) *ATG5* ($n = 3$ different cell strains), (**d**) *ATG7* ($n = 3$ different cell strains), (**e**) *NFE2L2* ($n = 4$ different cell strains), and (**f**) *SQSTM1* ($n = 4$ different cell strains) were analysed by RT-qPCR. Data represent mean ± SEM. Statistical significance (unpaired Student's t-test) relative to vehicle control is indicated by *($P < 0.05$) and **($P < 0.01$). Tre: trehalose; C: vehicle control.

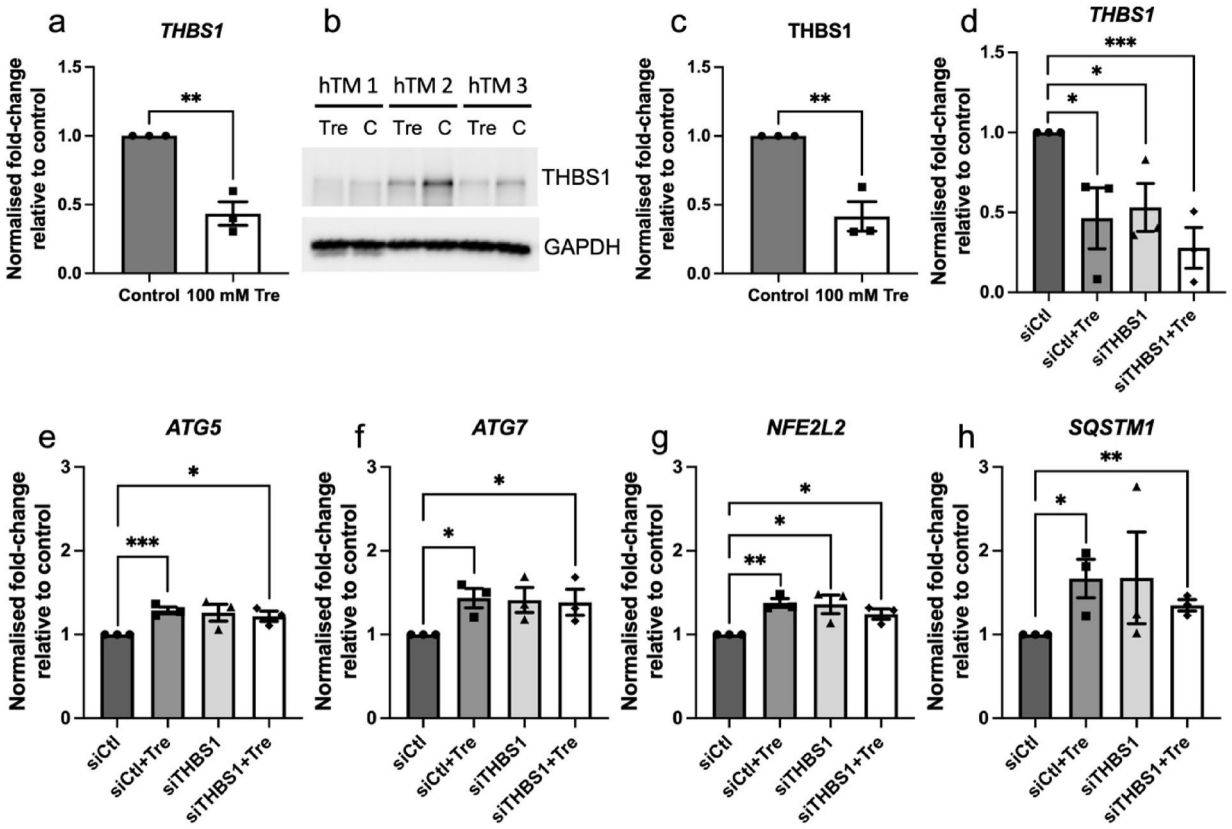

Fig. 3. Trehalose induced autophagy-associated gene expression through reducing THBS1 expression and function in hTM cells. To study the effect of trehalose on THBS1 expression, cultured hTM cells were treated with 100 mM trehalose and vehicle control for 48 h. Quantification of relative mRNA levels was performed by RT-qPCR, and western blot was used for quantification of protein levels. (**a**) Trehalose (100 mM) reduced *THBS1* mRNA expression by 57% in hTM cells. (**b**) Representative of three individual western blots of THSB1 expression in hTM cells after trehalose treatment. The original blot is presented in Supplementary Fig. S5. (**c**) The normalised THBS1 protein level ($n = 3$ different cell strains) as shown in (**b**). Trehalose (100 mM) reduced THBS1 protein level by 58% in hTM cells. To investigate the relevance of THBS1 in trehalose-induced autophagy in hTM cells, cultured hTM cells were transfected with 100 pmol of siCtl or siTHBS1 for 24 h, followed by 48 h of 100 mM trehalose treatment. Gene expression of (**d**) *THBS1*, (**e**) *ATG5*, (**f**) *ATG7*, (**g**) *NFE2L2* and (**h**) *SQSTM1* in siCtl- and siTHBS1-silenced hTM cells, with or without trehalose treatment, were evaluated by RT-qPCR. Data represent mean ± SEM. Statistical significance relative to vehicle control (unpaired Student's t-test) is indicated by *($P < 0.05$), ***($P < 0.01$) and ***($P < 0.001$). Tre: trehalose; siCtl: negative control siRNA; siTHBS1: THBS1-siRNA.

previous study[21], THBS1-siRNA (siTHBS1) significantly downregulated *THBS1* transcript levels by 47% ($P = 0.0358$, Fig. 3d) in hTM cells when compared with the negative control siRNA (siCtl). *THBS1* transcript levels in siTHBS1-treated cells were similar to transcript levels in cells treated with both siCtl and trehalose. Combined treatment with siTHBS1 and trehalose resulted in an additional reduction of *THBS1* transcript levels, though statistically insignificant. Further studies are needed to confirm this plausible trend. Interestingly, trehalose significantly increased the transcript levels of *ATG5* ($P = 0.0020$; Fig. 3e), *ATG7* ($P = 0.0201$; Fig. 3f), *NFE2L2* ($P = 0.0019$; Fig. 3g), and *SQSTM1* ($P = 0.0431$; Fig. 3h) in siCtl-treated hTM cells. The effect of siTHBS1 on transcript levels of ATGs was similar to the effect in cells treated with both siCtl and trehalose. Combined treatment with siTHBS1 and trehalose did not result in additive effects on transcript levels of ATGs (Fig. 3e, f, g and h). The lack of additive effects of siTHBS1 and trehalose on transcript levels of ATGs indicated that the effects of trehalose were mediated by reducing *THBS1* transcript levels.

Next, to assess the status of autophagy not only through mRNA and protein levels of ATGs, we also directly measured the presence of autophagic vacuoles in hTM cells in the presence and absence of trehalose and/or THBS1 inhibitor peptides using a fluorescent dye selectively labeling autophagic vacuoles. Trehalose upregulated autophagic vacuoles by 32% in hTM cells compared to the vehicle control ($P = 0.0019$; Fig. 4a). The THBS1 selective inhibitor LSKL peptide also upregulated autophagic vacuoles by 26% at 1 µM ($P = 0.0004$) and up to 55% at 5 µM ($P = 0.0020$) when compared with the control SLLK peptide (Fig. 4b). Trehalose could not further upregulate the autophagic vacuoles in hTM treated with 5 µM LSKL peptide (Fig. 4c), confirming that trehalose induced autophagy by regulating THBS1 expression and function in hTM cells.

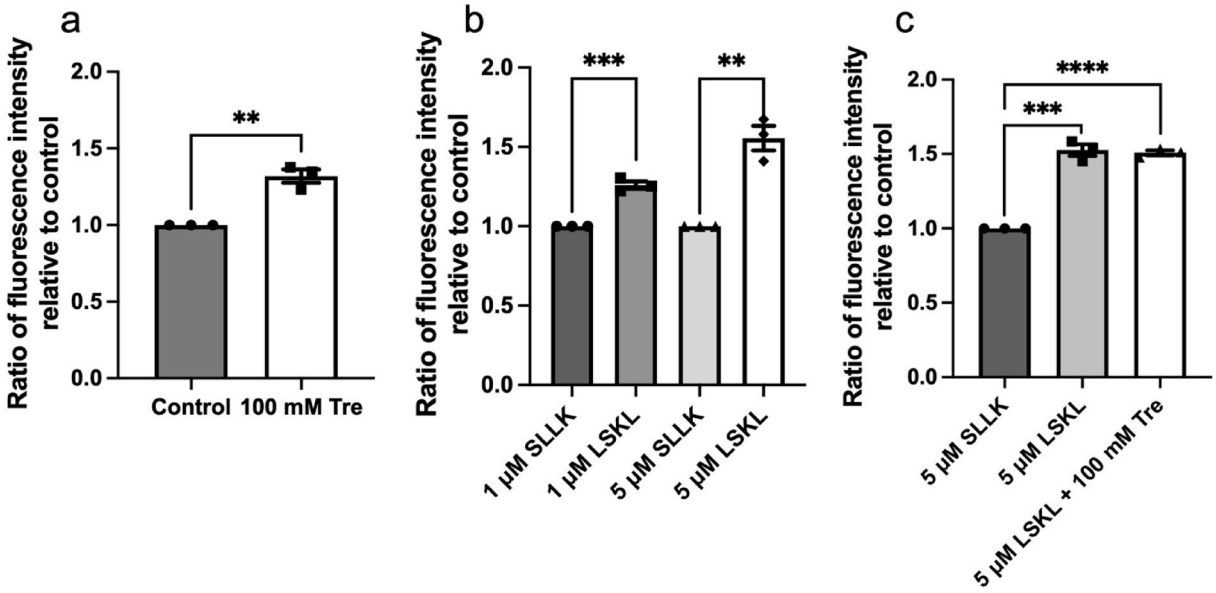

Fig. 4. Trehalose or THBS1 LSKL peptide upregulated autophagic flux in hTM cells. hTM cells were either incubated individually with trehalose (100 mM), SLLK or LSKL peptide (1 or 5 μM), or co-incubated with 100 mM trehalose and 5 μM LSKL peptide for 48 h. (**a**) 100 mM trehalose upregulated autophagic vacuoles in hTM cells by 32%. (**b**) THBS1 LSKL inhibitor peptide upregulated autophagic flux by 26% at 1 μM and 55% at 5 μM when compared with the SLLK control peptide. (**c**) Trehalose added to 5 μM LSKL peptide did not further upregulate autophagic vacuoles relative to cells treated with LSKL alone (51% and 53% upregulation, respectively). Data represent mean ± SEM ($n = 3$ different cell strains per group). Statistical significance relative to vehicle control (unpaired Student's t-test) is indicated by **($P < 0.01$), ***($P < 0.001$) and ***($P < 0.0001$). Tre: trehalose.

Discussion

Trehalose is a natural disaccharide and a prototypical autophagy inducer[45,57–60]. This study demonstrated that trehalose significantly increased outflow facility ex vivo and reduced IOP in vivo. Maltose, a disaccharide lacking the ability to induce autophagy[38], had no effects on outflow facility regulation ex vivo (Supplementary Fig. S7), ruling out the potential hyperosmotic effects of disaccharide. Forty-eight-hour incubation of trehalose induced autophagy and transcriptionally upregulated ATGs, including *ATG5*, *ATG7*, and *NFE2L2* in hTM cells. Our data also revealed that trehalose activated autophagy by downregulating THBS1 in hTM cells, corroborating the results of other researchers in retinal tissue[61,62]. Inhibition of THBS1 expression or function also upregulated autophagy-associated gene expression and autophagy flux. Importantly, trehalose did not additively activate autophagy when THBS1 is silenced or functionally inhibited, indicating that trehalose regulated autophagy through THBS1 suppression. These findings strongly suggested THBS1 acted as a mediator in trehalose-mediated autophagic regulation and likely also for aqueous humor outflow and IOP homeostasis.

Autophagy is an intracellular catabolic process in which cellular components are degraded or recycled to maintain cellular homeostasis. Several studies have examined the role of autophagy in glaucoma[29,31] and found that glaucoma is associated with autophagy-related gene mutations[63]. TM cells play an essential role in regulating aqueous humor outflow and maintaining IOP. Activation of autophagy by mechanical and oxidative stresses in TM protects TM cells from damage and cell death[23,34]. Dysregulation of autophagy in TM may increase the risk of glaucoma[32,33]. Prolonged corticosteroid treatment, such as DEX, leads to elevation of IOP, damage of the optic nerve, and eventually glaucoma if left untreated[6,7]. Recent studies showed that DEX upregulates THBS1 expression[19] and induces dysregulation of autophagy[22,24] in TM cells. Our findings strongly suggested that trehalose-induced autophagy provided a protective effect against corticosteroid-induced glaucomatous IOP elevation through suppression of THBS1 expression. Our results provided a rationale for clinical studies testing trehalose or other autophagy enhancers as therapeutic agents for the treatment of specific glaucoma sub-types.

Trehalose is a promising autophagy inducer as rapamycin (Rapa). Rapa is a potent autophagy inducer by inhibiting the kinase activity of target of rapamycin (TOR) proteins in various cell types and species, including yeast[64], mammalian lymphoma cells[65], neuron-like cells[66,67] and mice[68]. Similar to trehalose, Rapa (50 μM) significantly increased outflow facility ex vivo, reduced IOP in vivo, transcriptionally downregulated *THBS1* but upregulated ATGs in vitro (Supplementary Fig. S8), and the effects were comparable between trehalose and Rapa. Rapa was more efficient in upregulating autophagy-associated genes in siTHBS1-silenced hTM cells than trehalose, and Rapa had no additive effects when combined with *THBS1* silencing (Supplementary Fig, S9). These findings further confirmed the importance of THBS1 in mediating autophagy, and subsequent regulation of aqueous humor outflow and IOP.

The finding that transcript levels of *SQSTM1*, a LC3II substrate, increased with trehalose treatment was paradoxical. In general, SQSTM1 protein levels inversely correlate with autophagic activity and accumulate in autophagy-deficient cells[53,54]. While some reports have shown that trehalose reduces SQSTM1 protein level in vitro[58,69,70] and in vivo[71,72], others have also demonstrated that trehalose induces both SQSTM1 gene and protein level in vitro[38,73,74]. Sahani et al. have reported that cellular starvation through lacking amino acid and serum induces an initial autophagic SQSTM1 degradation in first two hours, followed by restoration of SQSTM1 protein level through enhanced SQSTM1 synthesis during the prolonged starvation[55]. The considerably long-lasting starvation during trehalose treatment (forty-eight hours) in our study may contribute to the dynamic changes in SQSTM1 level along with trehalose-induced autophagy. Trehalose started to increase *SQSTM1* gene level at 6-hour post-treatment and significantly increased to 4-fold at forty-eight hours (Supplementary Fig. S10). A similar change in SQSTM1 level upon trehalose treatment is also observed in other studies[38,62]. In any case, the increase in autophagic vacuoles, together with increased levels of ATG, unambiguously indicated autophagy induction with trehalose treatment.

In the current study, we found that trehalose-mediated autophagy activation reduced IOP and, therefore, likely protected against ocular hypertension or glaucoma. Similar effects have previously been observed in TM cells[23,32–34]. However, in contrast to our current study, some researchers have proposed that autophagy deficiency protects against glaucoma in mouse models[75,76]. This discrepancy may be due to the dual roles of autophagy in cell survival and death[77–79]. IOP elevation remains a significant risk factor and therapeutic target for glaucoma. It has become increasingly clear that IOP elevation might be the factor triggering RGCs dysfunction. Several evidence has shown that IOP elevation could exert mechanical stress on RGCs and their axons[80], and cause mitochondrial dysfunction in RGCs by reducing blood flow and inducing hypoxia[81]. Rodriguez-Muela et al.. have reported that autophagy inhibits apoptosis and hence promotes cell survival of RGCs in the mouse optic nerve axotomy model[82]. In contrast, Park et al.. have proposed that autophagy promotes apoptosis and cell death of RGCs in a chronic glaucoma rat model[83]. The dual role of autophagy strongly depends on its closely linked relationship with apoptosis. Autophagy and apoptosis share some common upstream signals[84] and may coexist in the same RGC in a rat model of retinal ischemia[85]. Autophagy is activated to allow cells to adapt to stress. Activation of autophagy may inhibit apoptosis and promote cell survival. However, overactivation of autophagy may stimulate apoptosis and promote apoptotic or autophagic cell death[86].

Another reason for conflicting findings may be the use of different models and cell types. In the spontaneous ocular hypertensive DBA/2J mouse model of glaucoma, overactivation of autophagy may be detrimental to RGCs and optic nerves[75,76]. In contrast, in TM cells, activation of autophagy protects against constant mechanical and oxidative stresses due to fluctuation of IOP or aging[23,34]. Porter *el al.* have reported that a static sustained mechanical stretch, mimicking acute IOP elevation, activates autophagy, induces the expression of LC3-II in TM cells as early as 30 min post-stretching[34]. Autophagosomes are increased in stretched TM cultures and high pressure-perfused porcine eyes[34]. This quick stretch-induced autophagy is mammalian TOR- (mTOR-) independent and is normal physiological response to maintain cellular functions and IOP homeostasis under mechanical stress[34]. However, the dysregulation of autophagy might contribute to cell death[75,76] or diseases[87]. Chronic oxidative stress impairs autophagy activation and reduce lysosomal degradation capacity in glaucomatous TM cells[32], which might contribute to the pathological changes, such as accumulation of autophagic vacuoles and pigments, in primary open-angled glaucoma[9,88,89]. While autophagy is generally protective, its regulation is crucial. Unbalanced autophagy can have detrimental effects. Researchers are actively studying the delicate balance of autophagy in TM cells, RGCs, and other ocular tissues. Understanding this balance may lead to novel therapeutic strategies for glaucoma control.

This study has potential limitations. Our findings demonstrated that trehalose activated autophagy by downregulating THBS1 in hTM cells, leading to the upregulation of autophagy-associated genes and autophagic flux. However, mouse models were adapted to study the effects of trehalose on outflow facility and IOP regulation. Despite mouse models are a common and valuable platform for exploring the pathophysiology of human diseases and potential drug candidates, the differences between the two species, particularly in genetics, physiology and immunology, might limit the ability of mouse models to recapitulate critical human disease pathophysiology and therapeutic responses, and the significance of data interpretation.

The variations in designs and procedures used in this study limit direct comparisons between different experiments. For example, the use of traditional 2-dimensional cultured hTM cells allows direct and straightforward study of the effects of trehalose on TM, but the limited representation of biological physiology may fail to illustrate precisely complex cellular environment. Ex vivo prefusion systems allow the study of ocular tissue with reduced complexity, but the semi-physiological representation may not be able to simulate its full functions within the body. Simple diffusion of trehalose was possible in hTM cells for quick preliminary study of trehalose, in which changes of trehalose-induced *SQSTM1* gene levels became noticeable at 6-hour post-treatment (Supplementary Fig. S10). Constant perfusion of trehalose enhanced its bioavailability to TM tissue with negligible loss induced THBS1 downregulation (Supplementary Fig. S6) and facilitated outflow facility (Fig. 1d) as soon as 4-hour perfusion.

However, the absorption of trehalose at TM tissue was relatively lower by i.p. injection or topical administration due to the loss during diffusion into surrounding tissues. Since topically applied drugs have a lower capacity of to penetrate the cornea, prolonged time might be needed to trigger the onset of trehalose-induced autophagy activation, which could be the explanation of the less pronounced changes in autophagy marker expression in mouse eyes at 3 h after trehalose topical application (Supplementary Fig. S11). This discrepancy gives rise to a major concern about the cause-and-effect relationship between trehalose-induced autophagy and THBS1. It is plausible that THBS1 acts as a mediator of trehalose-induced autophagy through interactions with autophagy-related proteins. Further studies are needed to confirm the cause-and-effect relationship between trehalose-induced autophagy and THBS1. Investigation of the effects of transient knock-out of autophagy-related genes

on THBS1 expression is particularly warranted. Monitoring of autophagy marker expression in TM tissues over extended period after trehalose topical application is also recommended.

The means of monitoring and measuring autophagy have to be carefully considered. Autophagic activity can be measured by monitoring the AP formation displaying punctate LC3-II, apart from autophagy flux assay. Electron microscopy offers high resolution and is a better tool to identify different autophagic structures along the pathway and measure autophagy activity qualitatively and quantitatively[90]. Comparisons should be made between animals of the same strain, age, gender and tissue to minimize the variations in tissue-specific basal autophagy[91] and autophagy marker expression[92–94]. Responses to autophagy induction may vary between individual animals[91] and different autophagy markers[95], emphasizing the needs of carefully considered experimental designs and sampling time.

In conclusion, our findings demonstrated that trehalose downregulated THBS1 and activated autophagy in TM cells, leading to increased outflow facility and reduced IOP. These data strongly suggested that trehalose-induced autophagy had a protective role against corticosteroid-induced glaucoma and supported that the worthwhileness of studying trehalose and other autophagy enhancers' experimental therapies for glaucoma.

Data availability

The source data for graphs analyzed in the study are available in the Supplementary Table S1. All other data are available from the corresponding author on reasonable request.

Received: 28 February 2025; Accepted: 1 October 2025
Published online: 06 November 2025

References

1. Pascolini, D. & Mariotti, S. P. Global estimates of visual impairment: 2010. *Br. J. Ophthalmol.* **96**, 614–618. https://doi.org/10.1136/bjophthalmol-2011-300539 (2012).
2. Tham, Y. C. et al. Global prevalence of glaucoma and projections of glaucoma burden through 2040: a systematic review and meta-analysis. *Ophthalmology* **121**, 2081–2090. https://doi.org/10.1016/j.ophtha.2014.05.013 (2014).
3. Becker, B. & Mills, D. W. Corticosteroids and intraocular pressure. *Arch. Ophthalmol.* **70**, 500–507. https://doi.org/10.1001/archopht.1963.00960050502012 (1963).
4. Fuchsjager-Mayrl, G. et al. Ocular blood flow and systemic blood pressure in patients with primary open-angle glaucoma and ocular hypertension. *Invest. Ophthalmol. Vis. Sci.* **45**, 834–839. https://doi.org/10.1167/iovs.03-0461 (2004).
5. Fuchshofer, R. & Tamm, E. R. The role of TGF-beta in the pathogenesis of primary open-angle glaucoma. *Cell. Tissue Res.* **347**, 279–290. https://doi.org/10.1007/s00441-011-1274-7 (2012).
6. Becker, B. & Mills, D. W. Elevated intraocular pressure following corticosteroid eye drops. *JAMA* **185**, 884–886. https://doi.org/10.1001/jama.1963.03060110088027 (1963).
7. Bernstein, H. N., Mills, D. W. & Becker, B. Steroid-induced elevation of intraocular pressure. *Arch. Ophthalmol.* **70**, 15–18. https://doi.org/10.1001/archopht.1963.00960050017005 (1963).
8. Kasetti, R. B., Maddineni, P., Millar, J. C., Clark, A. F. & Zode, G. S. Increased synthesis and deposition of extracellular matrix proteins leads to Endoplasmic reticulum stress in the trabecular meshwork. *Sci. Rep.* **7**, 14951. https://doi.org/10.1038/s41598-017-14938-0 (2017).
9. Tektas, O. Y. & Lutjen-Drecoll, E. Structural changes of the trabecular meshwork in different kinds of glaucoma. *Exp. Eye Res.* **88**, 769–775. https://doi.org/10.1016/j.exer.2008.11.025 (2009).
10. Overby, D. R. & Clark, A. F. Animal models of glucocorticoid-induced glaucoma. *Exp. Eye Res.* **141**, 15–22. https://doi.org/10.1016/j.exer.2015.06.002 (2015).
11. Mohd Nasir, N. A., Agarwal, R., Krasilnikova, A., Sheikh Abdul Kadir, S. H. & Iezhitsa, I. Effect of trans-resveratrol on dexamethasone-induced changes in the expression of MMPs by human trabecular meshwork cells: involvement of adenosine A(1) receptors and NFkB. *Eur. J. Pharmacol.* **887**, 173431. https://doi.org/10.1016/j.ejphar.2020.173431 (2020).
12. el-Shabrawi, Y. et al. Synthesis pattern of matrix metalloproteinases (MMPs) and inhibitors (TIMPs) in human explant organ cultures after treatment with latanoprost and dexamethasone. *Eye (Lond)* 14 (Pt 3A), 375–383 (2000). https://doi.org/10.1038/eye.2000.92
13. Raghunathan, V. K. et al. Dexamethasone stiffens trabecular meshwork, trabecular meshwork Cells, and matrix. *Invest. Ophthalmol. Vis. Sci.* **56**, 4447–4459. https://doi.org/10.1167/iovs.15-16739 (2015).
14. Peng, M. et al. Cross-linked actin networks (CLANs) affect stiffness and/or actin dynamics in Transgenic transformed and primary human trabecular meshwork cells. *Exp. Eye Res.* **220**, 109097. https://doi.org/10.1016/j.exer.2022.109097 (2022).
15. Yuan, Y. et al. Dexamethasone induces cross-linked actin networks in trabecular meshwork cells through noncanonical Wnt signaling. *Invest. Ophthalmol. Vis. Sci.* **54**, 6502–6509. https://doi.org/10.1167/iovs.13-12447 (2013).
16. Li, G. et al. In vivo measurement of trabecular meshwork stiffness in a corticosteroid-induced ocular hypertensive mouse model. *Proc. Natl. Acad. Sci. U S A.* **116**, 1714–1722. https://doi.org/10.1073/pnas.1814889116 (2019).
17. Overby, D. R. et al. Ultrastructural changes associated with dexamethasone-induced ocular hypertension in mice. *Invest. Ophthalmol. Vis. Sci.* **55**, 4922–4933. https://doi.org/10.1167/iovs.14-14429 (2014).
18. Ren, R., Humphrey, A. A., Swain, D. L. & Gong, H. Relationships between intraocular Pressure, effective filtration Area, and morphological changes in the trabecular meshwork of Steroid-Induced ocular hypertensive mouse eyes. *Int. J. Mol. Sci.* **23** https://doi.org/10.3390/ijms23020854 (2022).
19. Shan, S. W. et al. New insight of common regulatory pathways in human trabecular meshwork cells in response to dexamethasone and prednisolone using an integrated quantitative proteomics: SWATH and MRM-HR mass spectrometry. *J. Proteome Res.* **16**, 3753–3765. https://doi.org/10.1021/acs.jproteome.7b00449 (2017).
20. Murphy-Ullrich, J. E., Schultz-Cherry, S. & Hook, M. Transforming growth factor-beta complexes with thrombospondin. *Mol. Biol. Cell.* **3**, 181–188. https://doi.org/10.1091/mbc.3.2.181 (1992).
21. Shan, S. W. et al. Thrombospondin-1 mediates Rho-kinase inhibitor-induced increase in outflow-facility. *J. Cell. Physiol.* **236**, 8226–8238. https://doi.org/10.1002/jcp.30492 (2021).
22. Sbardella, D., Tundo, G. R., Coletta, M., Manni, G. & Oddone, F. Dexamethasone downregulates autophagy through accelerated Turn-Over of the Ulk-1 complex in a trabecular meshwork cells strain: insights on Steroid-Induced glaucoma pathogenesis. *Int. J. Mol. Sci.* **22** https://doi.org/10.3390/ijms22115891 (2021).
23. He, J. N. et al. Rapamycin removes damaged mitochondria and protects human trabecular meshwork (TM-1) cells from chronic oxidative stress. *Mol. Neurobiol.* **56**, 6586–6593. https://doi.org/10.1007/s12035-019-1559-5 (2019).
24. Zhu, X. et al. Protective effects of Rapamycin on trabecular meshwork cells in Glucocorticoid-Induced glaucoma mice. *Front. Pharmacol.* **11**, 1006. https://doi.org/10.3389/fphar.2020.01006 (2020).

25. Mizushima, N. Autophagy: process and function. *Genes Dev.* **21**, 2861–2873. https://doi.org/10.1101/gad.1599207 (2007).
26. Nixon, R. A. The role of autophagy in neurodegenerative disease. *Nat. Med.* **19**, 983–997. https://doi.org/10.1038/nm.3232 (2013).
27. Schneider, J. L. & Cuervo, A. M. Autophagy and human disease: emerging themes. *Curr. Opin. Genet. Dev.* **26**, 16–23. https://doi.org/10.1016/j.gde.2014.04.003 (2014).
28. Tan, C. C. et al. Autophagy in aging and neurodegenerative diseases: implications for pathogenesis and therapy. *Neurobiol. Aging.* **35**, 941–957. https://doi.org/10.1016/j.neurobiolaging.2013.11.019 (2014).
29. Adornetto, A. et al. The role of autophagy in glaucomatous optic neuropathy. *Front. Cell. Dev. Biol.* **8**, 121. https://doi.org/10.3389/fcell.2020.00121 (2020).
30. Garnock-Jones, K. P. Ripasudil: first global approval. *Drugs* **74**, 2211–2215. https://doi.org/10.1007/s40265-014-0333-2 (2014).
31. Hirt, J. & Liton, P. B. Autophagy and mechanotransduction in outflow pathway cells. *Exp. Eye Res.* **158**, 146–153. https://doi.org/10.1016/j.exer.2016.06.021 (2017).
32. Porter, K., Hirt, J., Stamer, W. D. & Liton, P. B. Autophagic dysregulation in glaucomatous trabecular meshwork cells. *Biochim. Biophys. Acta*. **1852**, 379–385. https://doi.org/10.1016/j.bbadis.2014.11.021 (2015).
33. Porter, K., Nallathambi, J., Lin, Y. & Liton, P. B. Lysosomal basification and decreased autophagic flux in oxidatively stressed trabecular meshwork cells: implications for glaucoma pathogenesis. *Autophagy* **9**, 581–594. https://doi.org/10.4161/auto.23568 (2013).
34. Porter, K. M., Jeyabalan, N. & Liton, P. B. MTOR-independent induction of autophagy in trabecular meshwork cells subjected to biaxial stretch. *Biochim. Biophys. Acta*. **1843**, 1054–1062. https://doi.org/10.1016/j.bbamcr.2014.02.010 (2014).
35. Chen, W. et al. Trehalose protects against ocular surface disorders in experimental murine dry eye through suppression of apoptosis. *Exp. Eye Res.* **89**, 311–318. https://doi.org/10.1016/j.exer.2009.03.015 (2009).
36. Argov, Z., Vornovitsky, H., Blumen, S. & Caraco, Y. (AAN Enterprises, (2015).
37. Tien, N. T., Karaca, I., Tamboli, I. Y. & Walter, J. Trehalose alters subcellular trafficking and the metabolism of the Alzheimer-associated amyloid precursor protein. *J. Biol. Chem.* **291**, 10528–10540. https://doi.org/10.1074/jbc.M116.719286 (2016).
38. Yoon, Y. S. et al. Is Trehalose an autophagic inducer? Unraveling the roles of non-reducing disaccharides on autophagic flux and alpha-synuclein aggregation. *Cell. Death Dis.* **8**, e3091. https://doi.org/10.1038/cddis.2017.501 (2017).
39. Snyder, R. W., Stamer, W. D., Kramer, T. R. & Seftor, R. E. Corticosteroid treatment and trabecular meshwork proteases in cell and organ culture supernatants. *Exp. Eye Res.* **57**, 461–468. https://doi.org/10.1006/exer.1993.1148 (1993).
40. Stamer, D. W., Roberts, B. C., Epstein, D. L. & Allingham, R. R. Isolation of primary open-angle glaucomatous trabecular meshwork cells from whole eye tissue. *Curr. Eye Res.* **20**, 347–350 (2000).
41. Stamer, W. D., Seftor, R. E., Williams, S. K., Samaha, H. A. & Snyder, R. W. Isolation and culture of human trabecular meshwork cells by extracellular matrix digestion. *Curr. Eye Res.* **14**, 611–617. https://doi.org/10.3109/02713689508998409 (1995).
42. Keller, K. E. et al. Consensus recommendations for trabecular meshwork cell isolation, characterization and culture. *Exp. Eye Res.* **171**, 164–173. https://doi.org/10.1016/j.exer.2018.03.001 (2018).
43. Richards, A. B. et al. Trehalose: a review of properties, history of use and human tolerance, and results of multiple safety studies. *Food Chem. Toxicol.* **40**, 871–898. https://doi.org/10.1016/s0278-6915(02)00011-x (2002).
44. Yang, Z. & Klionsky, D. J. An overview of the molecular mechanism of autophagy. *Curr. Top. Microbiol. Immunol.* **335**, 1–32. https://doi.org/10.1007/978-3-642-00302-8_1 (2009).
45. Del Bello, B., Gamberucci, A., Marcolongo, P. & Maellaro, E. The autophagy inducer Trehalose stimulates macropinocytosis in NF1-deficient glioblastoma cells. *Cancer Cell. Int.* **22**, 232. https://doi.org/10.1186/s12935-022-02652-5 (2022).
46. Yoshii, S. R. & Mizushima, N. Monitoring and measuring autophagy. *Int. J. Mol. Sci.* **18** https://doi.org/10.3390/ijms18091865 (2017).
47. Liu, J. et al. Nrf2 and its dependent autophagy activation cooperatively counteract ferroptosis to alleviate acute liver injury. *Pharmacol. Res.* **187**, 106563. https://doi.org/10.1016/j.phrs.2022.106563 (2023).
48. Pajares, M. et al. Transcription factor NFE2L2/NRF2 is a regulator of macroautophagy genes. *Autophagy* **12**, 1902–1916. https://doi.org/10.1080/15548627.2016.1208889 (2016).
49. Komatsu, M. et al. The selective autophagy substrate p62 activates the stress responsive transcription factor Nrf2 through inactivation of Keap1. *Nat. Cell. Biol.* **12**, 213–223. https://doi.org/10.1038/ncb2021 (2010).
50. De Plano, L. M., Calabrese, G., Rizzo, M. G., Oddo, S. & Caccamo, A. The Role of the Transcription Factor Nrf2 in Alzheimer's Disease: Therapeutic Opportunities. *Biomolecules* **13** https://doi.org/10.3390/biom13030549 (2023).
51. Bjorkoy, G. et al. p62/SQSTM1 forms protein aggregates degraded by autophagy and has a protective effect on huntingtin-induced cell death. *J. Cell. Biol.* **171**, 603–614. https://doi.org/10.1083/jcb.200507002 (2005).
52. Mizushima, N. & Komatsu, M. Autophagy: renovation of cells and tissues. *Cell* **147**, 728–741. https://doi.org/10.1016/j.cell.2011.10.026 (2011).
53. Komatsu, M. et al. Homeostatic levels of p62 control cytoplasmic inclusion body formation in autophagy-deficient mice. *Cell* **131**, 1149–1163. https://doi.org/10.1016/j.cell.2007.10.035 (2007).
54. Nakai, A. et al. The role of autophagy in cardiomyocytes in the basal state and in response to hemodynamic stress. *Nat. Med.* **13**, 619–624. https://doi.org/10.1038/nm1574 (2007).
55. Sahani, M. H., Itakura, E. & Mizushima, N. Expression of the autophagy substrate SQSTM1/p62 is restored during prolonged starvation depending on transcriptional upregulation and autophagy-derived amino acids. *Autophagy* **10**, 431–441. https://doi.org/10.4161/auto.27344 (2014).
56. Flugel-Koch, C., Ohlmann, A., Fuchshofer, R., Welge-Lussen, U. & Tamm, E. R. Thrombospondin-1 in the trabecular meshwork: localization in normal and glaucomatous eyes, and induction by TGF-beta1 and dexamethasone in vitro. *Exp. Eye Res.* **79**, 649–663. https://doi.org/10.1016/j.exer.2004.07.005 (2004).
57. Aguib, Y. et al. Autophagy induction by Trehalose counteracts cellular prion infection. *Autophagy* **5**, 361–369. https://doi.org/10.4161/auto.5.3.7662 (2009).
58. Casarejos, M. J. et al. The accumulation of neurotoxic proteins, induced by proteasome inhibition, is reverted by trehalose, an enhancer of autophagy, in human neuroblastoma cells. *Neurochem Int.* **58**, 512–520. https://doi.org/10.1016/j.neuint.2011.01.008 (2011).
59. Sarkar, S., Davies, J. E., Huang, Z., Tunnacliffe, A. & Rubinsztein, D. C. Trehalose, a novel mTOR-independent autophagy enhancer, accelerates the clearance of mutant Huntingtin and alpha-synuclein. *J. Biol. Chem.* **282**, 5641–5652. https://doi.org/10.1074/jbc.M609532200 (2007).
60. Tanji, K. et al. Trehalose intake induces chaperone molecules along with autophagy in a mouse model of lewy body disease. *Biochem. Biophys. Res. Commun.* **465**, 746–752. https://doi.org/10.1016/j.bbrc.2015.08.076 (2015).
61. Lotfi, P. et al. Trehalose reduces retinal degeneration, neuroinflammation and storage burden caused by a lysosomal hydrolase deficiency. *Autophagy* **14**, 1419–1434. https://doi.org/10.1080/15548627.2018.1474313 (2018).
62. Rusmini, P. et al. Trehalose induces autophagy via lysosomal-mediated TFEB activation in models of motoneuron degeneration. *Autophagy* **15**, 631–651. https://doi.org/10.1080/15548627.2018.1535292 (2019).
63. Mizushima, N. & Levine, B. Autophagy in human diseases. *N Engl. J. Med.* **383**, 1564–1576. https://doi.org/10.1056/NEJMra2022774 (2020).
64. Noda, T., Ohsumi, Y. & Tor A phosphatidylinositol kinase homologue, controls autophagy in yeast. *J. Biol. Chem.* **273**, 3963–3966. https://doi.org/10.1074/jbc.273.7.3963 (1998).

65. Sabers, C. J. et al. Isolation of a protein target of the FKBP12-rapamycin complex in mammalian cells. *J. Biol. Chem.* **270**, 815–822. https://doi.org/10.1074/jbc.270.2.815 (1995).
66. Ravikumar, B., Duden, R. & Rubinsztein, D. C. Aggregate-prone proteins with polyglutamine and polyalanine expansions are degraded by autophagy. *Hum. Mol. Genet.* **11**, 1107–1117. https://doi.org/10.1093/hmg/11.9.1107 (2002).
67. Ravikumar, B. et al. Inhibition of mTOR induces autophagy and reduces toxicity of polyglutamine expansions in fly and mouse models of huntington disease. *Nat. Genet.* **36**, 585–595. https://doi.org/10.1038/ng1362 (2004).
68. Rangaraju, S. et al. Rapamycin activates autophagy and improves myelination in explant cultures from neuropathic mice. *J. Neurosci.* **30**, 11388–11397. https://doi.org/10.1523/JNEUROSCI.1356-10.2010 (2010).
69. Ma, Z. et al. Trehalose enhances macrophage autophagy to promote Myelin debris clearance after spinal cord injury. *Cell. Biosci.* **15**, 11. https://doi.org/10.1186/s13578-025-01357-2 (2025).
70. Xu, C., Chen, X., Sheng, W. B. & Yang, P. Trehalose restores functional autophagy suppressed by high glucose. *Reprod. Toxicol.* **85**, 51–58. https://doi.org/10.1016/j.reprotox.2019.02.005 (2019).
71. Castillo, K. et al. Trehalose delays the progression of amyotrophic lateral sclerosis by enhancing autophagy in motoneurons. *Autophagy* **9**, 1308–1320. https://doi.org/10.4161/auto.25188 (2013).
72. Rodriguez-Navarro, J. A. et al. Trehalose ameliorates dopaminergic and Tau pathology in parkin deleted/tau overexpressing mice through autophagy activation. *Neurobiol. Dis.* **39**, 423–438. https://doi.org/10.1016/j.nbd.2010.05.014 (2010).
73. Abokyi, S., Shan, S. W., To, C. H., Chan, H. H. & Tse, D. Y. Autophagy Upregulation by the TFEB Inducer Trehalose Protects against Oxidative Damage and Cell Death Associated with NRF2 Inhibition in Human RPE Cells. *Oxid Med Cell Longev* 5296341 (2020). (2020). https://doi.org/10.1155/2020/5296341
74. Kobayashi, M. et al. Trehalose induces SQSTM1/p62 expression and enhances lysosomal activity and antioxidative capacity in adipocytes. *FEBS Open. Bio.* **11**, 185–194. https://doi.org/10.1002/2211-5463.13055 (2021).
75. Dixon, A. et al. Autophagy deficiency protects against ocular hypertension and neurodegeneration in experimental and spontanous glaucoma mouse models. *Cell. Death Dis.* **14**, 554. https://doi.org/10.1038/s41419-023-06086-3 (2023).
76. Hirt, J., Porter, K., Dixon, A., McKinnon, S. & Liton, P. B. Contribution of autophagy to ocular hypertension and neurodegeneration in the DBA/2J spontaneous glaucoma mouse model. *Cell. Death Discov.* **4**, 14. https://doi.org/10.1038/s41420-018-0077-y (2018).
77. Chaabane, W. et al. Autophagy, apoptosis, mitoptosis and necrosis: interdependence between those pathways and effects on cancer. *Arch. Immunol. Ther. Exp. (Warsz).* **61**, 43–58. https://doi.org/10.1007/s00005-012-0205-y (2013).
78. Subramani, S. & Malhotra, V. Non-autophagic roles of autophagy-related proteins. *EMBO Rep.* **14**, 143–151. https://doi.org/10.1038/embor.2012.220 (2013).
79. Yu, L., Lenardo, M. J. & Baehrecke, E. H. Autophagy and caspases: a new cell death program. *Cell. Cycle.* **3**, 1124–1126 (2004).
80. Chen, D. et al. Regulated necrosis in glaucoma: focus on ferroptosis and pyroptosis. *Mol. Neurobiol.* **61**, 2542–2555. https://doi.org/10.1007/s12035-023-03732-x (2024).
81. Zhao, W. J. et al. Regulated cell death of retinal ganglion cells in glaucoma: molecular insights and therapeutic potentials. *Cell. Mol. Neurobiol.* **43**, 3161–3178. https://doi.org/10.1007/s10571-023-01373-1 (2023).
82. Rodriguez-Muela, N., Germain, F., Marino, G., Fitze, P. S. & Boya, P. Autophagy promotes survival of retinal ganglion cells after optic nerve axotomy in mice. *Cell. Death Differ.* **19**, 162–169. https://doi.org/10.1038/cdd.2011.88 (2012).
83. Park, H. Y., Kim, J. H. & Park, C. K. Activation of autophagy induces retinal ganglion cell death in a chronic hypertensive glaucoma model. *Cell. Death Dis.* **3**, e290. https://doi.org/10.1038/cddis.2012.26 (2012).
84. Maiuri, M. C., Zalckvar, E., Kimchi, A. & Kroemer, G. Self-eating and self-killing: crosstalk between autophagy and apoptosis. *Nat. Rev. Mol. Cell. Biol.* **8**, 741–752. https://doi.org/10.1038/nrm2239 (2007).
85. Piras, A., Gianetto, D., Conte, D., Bosone, A. & Vercelli, A. Activation of autophagy in a rat model of retinal ischemia following high intraocular pressure. *PLoS One.* **6**, e22514. https://doi.org/10.1371/journal.pone.0022514 (2011).
86. Wang, Y., Huang, C., Zhang, H. & Wu, R. Autophagy in glaucoma: crosstalk with apoptosis and its implications. *Brain Res. Bull.* **117**, 1–9. https://doi.org/10.1016/j.brainresbull.2015.06.001 (2015).
87. Tanabe, F. et al. Accumulation of p62 in degenerated spinal cord under chronic mechanical compression: functional analysis of p62 and autophagy in hypoxic neuronal cells. *Autophagy* **7**, 1462–1471. https://doi.org/10.4161/auto.7.12.17892 (2011).
88. Cracknell, K. P. et al. Melanin in the trabecular meshwork is associated with age, POAG but not Latanoprost treatment. A masked morphometric study. *Exp. Eye Res.* **82**, 986–993. https://doi.org/10.1016/j.exer.2005.10.009 (2006).
89. Rohen, J. W. Presence of matrix vesicles in the trabecular meshwork of glaucomatous eyes. *Graefes Arch. Clin. Exp. Ophthalmol.* **218**, 171–176. https://doi.org/10.1007/BF02150090 (1982).
90. Jung, M., Choi, H. & Mun, J. Y. The autophagy research in electron microscopy. *Appl. Microsc.* **49**, 11. https://doi.org/10.1186/s42649-019-0012-6 (2019).
91. Moulis, M. & Vindis, C. Methods for measuring autophagy in mice. *Cells* **6** https://doi.org/10.3390/cells6020014 (2017).
92. Klionsky, D. J. et al. Guidelines for the use and interpretation of assays for monitoring autophagy in higher eukaryotes. *Autophagy* **4**, 151–175. https://doi.org/10.4161/auto.5338 (2008).
93. Pulliero, A. et al. Oxidative damage and autophagy in the human trabecular meshwork as related with ageing. *PLoS One.* **9**, e98106. https://doi.org/10.1371/journal.pone.0098106 (2014).
94. Nettesheim, A. et al. Autophagy in the aging and experimental ocular hypertensive mouse model. *Invest. Ophthalmol. Vis. Sci.* **61**, 31. https://doi.org/10.1167/iovs.61.10.31 (2020).
95. Mizushima, N. & Yoshimori, T. How to interpret LC3 Immunoblotting. *Autophagy* **3**, 542–545. https://doi.org/10.4161/auto.4600 (2007).

Acknowledgements

This work was supported by The Hong Kong Polytechnic University (PolyU Internal Grant: 1-BD6R and 1-BBDL), the InnoHK initiative of the Innovation and Technology Commission of the Hong Kong Special Administrative Region Government, and the Health Medical Research Fund (08191556, 09200276 and 20212781). We thank the University Research Facility in Life Sciences (ULS) and the University Behavioral and Systems Neuroscience (UBSN), The Hong Kong Polytechnic University, for providing and maintaining the equipment needed for Real time-quantitative PCR, flow cytometry apparatus and confocal microscopy. We also thank the Centralized Animal Facilities, The Hong Kong Polytechnic University, for providing the animal husbandry service.

Author contributions

C.L. performed experiments and analysed the data. K.C. performed the experiments, analysed and interpreted the data, and wrote the manuscript. H.L. and C.T. performed experiments. W.Y. performed experiments and reviewed the manuscript. N.W. performed the experiments. W.D.S. planned experiments, contributed resources and reviewed the manuscript. C.D. and D.Y.T. planned experiments, acquired funding and reviewed the manuscript. S.S.S. provided supervision, planned experiments, acquired funding, analysed and interpreted the data, and reviewed the manuscript.

Declarations

Competing interests
The authors declare no competing interests.

Additional information
Supplementary Information The online version contains supplementary material available at https://doi.org/10.1038/s41598-025-22873-8.

Correspondence and requests for materials should be addressed to D.Y.-y.T. or S.S.-w.S.

Reprints and permissions information is available at www.nature.com/reprints.

Publisher's note Springer Nature remains neutral with regard to jurisdictional claims in published maps and institutional affiliations.